DESIGN OF AN OUTPUT FEEDBACK TRAJECTORY CONTROLLER FOR AN AUTOMATED GUIDED VEHICLE

GEOVANY A. BORGES

Département de Robotique
LIRMM, UMR CNRS/Université Montpellier II, n°. C55060
161, rue ADA. 34392 - Montpellier - Cedex 5 - France
E-mail: borges@lirmm.fr

ANTONIO M. N. LIMA AND GURDIP S. DEEP

Departamento de Engenharia Elétrica, Universidade Federal da Paraíba
UFPB/CCT/DEE - Campus II
Caixa Postal 10.004
58109-970 Campina Grande, PB, Brazil
E-mail: {amnlima,deep}@dee.ufpb.br

Abstract— This paper presents the design of an output feedback trajectory controller for a Automated Guided Vehicle (AGV) differential drive. Its control architecture assumes that the two drive wheels are not coupled and the vehicle dynamics is not taken into account. It employs two independent velocity controllers that ensure the wheels' velocities referenced by the trajectory controller. The reference trajectory is painted on the ground and is composed only by line segments and soft arcs. Simulation and experimental results show the satisfactory tracking performance of the proposed controller.

Key Words— Robot control; mobile robots; nonlinear systems; trajectory tracking; control schemes.

1 Introduction

The problem of trajectory control of mobile platforms has been extensively reported in the literature during this decade and different solutions for automated guided vehicles (AGVs) or autonomous vehicles (AVs) have been investigated. In general, this kind of problem does not depend upon the manner in which the vehicle trajectory is specified. The trajectory may be either physically marked on the floor to serve as a guide or may be defined in terms of elapsed time intervals since the initiation of the vehicle movement. However, the propulsion method employed in the vehicle has a decisive influence in the design and implementation of the trajectory control scheme.

In order to follow a given trajectory, a mobile robot must be equipped with a trajectory controller and a sensor for measuring the vehicle deviation from the marked trajectory. Its main purpose is to reduce the vehicle's measured deviation from the marked trajectory to zero. This deviation can be defined in terms of linear displacement and angular deviation from the marked trajectory. The control action should, in principle, be dependent on the vehicle speed. It is well established that smooth PID controllers or those based on state feedback do not guarantee stability for non-holonomic systems (Zhang et al., 1997) and differential drive-based vehicles belong to this class of systems. However, for simpler trajectories composed of only linear segments and soft arcs which are commonly employed for AGVs, these kind of controllers should yield satisfactory results (Cox, 1991). For ensuring global stability for any arbitrary trajectory, it becomes necessary to employ nonlinear control techniques. The more often employed control strategies are based on nonlinear state feedback (Zhang et al., 1997; d'Andréa Novel et al., 1995; Aguilar et al., 1998), adaptive control (Colbaugh et al., 1998; Mazur and Hossa, 1997) and fuzzy logic (Tso et al., 1996; Fung and Tso, 1998).

The trajectory controller presented in this paper has been designed for an AGV which should track a marked trajectory consisting of soft arcs and linear segments. Its design is original in the sense that the controller parameters are analytically determined as a function of the vehicle parameters and of the desired trajectory error behaviour.

This paper is organized as follows. The kinematics of a differential drive vehicle is presented in Section 2. Section 3 presents the variables used to quantify the trajectory deviation and the sensor used to estimate such variables. Section 4 presents the design of the control system. Simulations and experimental results are presented in Sections 5 and 6, respectively. The conclusion of this investigation is presented in Section 7.

2 Vehicle kinematics

The AGV used in the present investigation is a prototype assembled in our laboratory that employs differential traction which consists of drive wheels coupled to two independent dc motors (see Figure 1). Two other caster wheels are provided for ensuring stability of the vehicle. The AGV was designed to track a fixed route. An optical marking in the form of a strip painted on the floor is the route guide or the marked trajectory. The color of the painted strip contrasts against that of

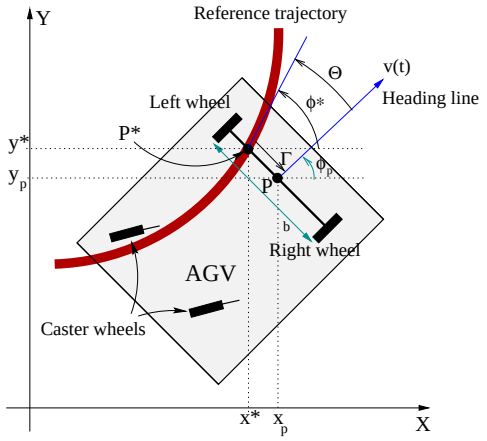

Figure 1. Defining trajectory error variables

the floor. In the experimental system, the route guide is painted black on the white floor.

The vehicle position P is defined to be (x_p, y_p) in the cartesian $X-Y$ plane where P is the mid-point position on the imaginary axle which connects the two drive wheels. The vehicle direction is measured in terms of the angle ϕ_p between the X axis and a line orthogonal to the drive wheels axle. Therefore, the vehicle position on the $X-Y$ plane is completely specified in terms of (x_p, y_p, ϕ_p). The drive wheels are referred as the right wheel and left wheel, in conformity with its location with respect to the line orthogonal to the drive wheels axle.

The differential equations that describe the dependence of the vehicle position with the angular speed of the drive wheels are as follows:

$$\dot{x}_p(t) = v(t)\cos\phi(t), \tag{1}$$

$$\dot{y}_p(t) = v(t)\sin\phi(t), \tag{2}$$

$$\dot{\phi}(t) = \frac{\omega_r(t) - \omega_l(t)}{b} r, \tag{3}$$

where for the prototype vehicle $r = 0.0325m$ is the radius of the drive wheels (assumed to be identical), $b = 0.275m$ is the distance between the drive wheels and ω_r and ω_l are the angular velocities of the right and left drive wheels respectively. The speed of the vehicle $v(t)$ is given by:

$$v(t) = \frac{\omega_r(t) + \omega_l(t)}{2} r. \tag{4}$$

3 Deviation from the marked trajectory

The deviation of the vehicle from the marked trajectory is specified in terms of two variables: linear orthogonal displacement Γ and angular deviation Θ as shown in Figure 1. The desired position of the vehicle on the reference trajectory is represented by the point $P^* = (x^*, y^*)$. P^* is the intersection point between the reference trajectory and the imaginary axle that connects the wheels. The orthogonal displacement Γ represents the distance $P - P^*$, being negative if P^* is to the right side of P on the imaginary axle. The angular deviation Θ is the angle between the tangent to the trajectory at P^* and the line orthogonal to the wheels baseline and that passes through P.

An optical sensor to measure these deviation variables has been reported by Borges *et al.* (Borges et al., 1998). In this report the effectiveness of the sensor performance has been determined using a specially designed test-platform. This effectiveness was evaluated using geometrical algorithms and one neural network-based algorithm. The neural algorithm gave the most accurate estimates for Γ and Θ, but its execution time is little higher than that of the purely geometrical algorithms. However, if the sensor's image acquisition time is taken into account the neural algorithm offers advantages over the other algorithms. The use of this optical sensor requires that Γ and Θ be restricted to

$$|\Theta| < \arctan\left(\frac{0.0478 - |\Gamma|}{0.032}\right), \tag{5}$$

and

$$|\Gamma| < 0.0478\ m. \tag{6}$$

4 Trajectory control

4.1 *Controller architecture*

In the applications related with the transport of materials on a shop floor, sudden changes in the vehicle speed may cause undesirable movement of the items being transported, due to inertial forces and the skidding of the vehicle. Thus one of the important attributes of a trajectory controller is to maintain the vehicle speed constant or should produce rather soft variations in the speed. To obtain constant speed on a curvilinear portion of the trajectory, the drive wheel angular speeds ω_r and ω_l of the right and left wheels respectively should be of the form:

$$\omega_r(t) = \frac{v_p}{r} + \Delta\omega(\Gamma(t), \Theta(t)), \tag{7}$$

$$\omega_l(t) = \frac{v_p}{r} - \Delta\omega(\Gamma(t), \Theta(t)), \tag{8}$$

Thus as per Eq. (4), the vehicle speed $v(t)$ is constant and given by $v(t) = v_p$. The differential term $\Delta\omega(\Gamma(t), \Theta(t))$ should correspond to curvilinear trajectory of the moving vehicle with an instantaneous curvature radius $R_c(t)$ given by:

$$R_c(t) = -\frac{\omega_r(t) + \omega_l(t)}{\omega_r(t) - \omega_l(t)} \frac{b}{2} = -\frac{v_p}{\Delta\omega(\Gamma(t), \Theta(t))} \frac{b}{2r} \tag{9}$$

Thus $\Delta\omega(\Gamma(t), \Theta(t))$ can be considered as the control variable in the AGV and is determined from variables $\Gamma(t)$ and $\Theta(t)$ describing the vehicle's deviation from the marked trajectory. The convention adopted in the present paper is that a left turn ($\omega_r(t) > \omega_l(t)$) implies $R_c(t) < 0$.

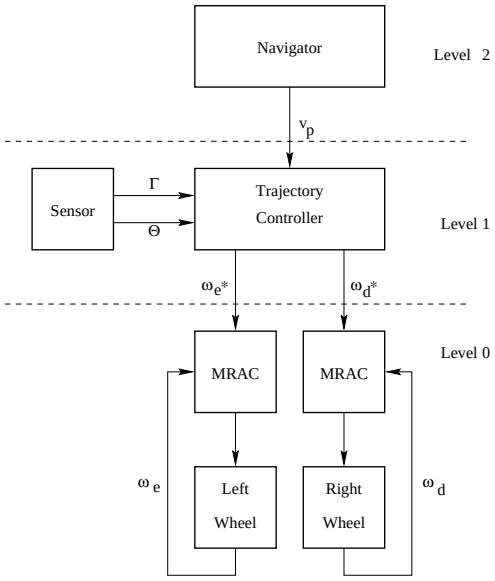

Figure 2. AGV's Hierarchical control organization.

The hierarchical organization of the controller operations is shown in Figure 2. There are three control levels: the navigation level (Level 2), the trajectory control level (Level 1), and the speed control level (Level 0). At first level the vehicles's desired cruising speed is defined or specified. At the second level, the reference speeds of the drive wheels are determined in order to keep the vehicle along a given trajectory. These reference angular speeds are given as per Eqs. (7) and (8) or by

$$\omega_r^*(t) = \frac{v_p}{r} + \Delta\omega(\Gamma(t),\Theta(t)), \tag{10}$$

$$\omega_l^*(t) = \frac{v_p}{r} - \Delta\omega(\Gamma(t),\Theta(t)). \tag{11}$$

At the lowest level two speed controllers are employed to make the drive wheels rotate at the reference speeds supplied by the immediately higher level. The wheels speed controller are based on the MRAC strategy and were designed via Lyapunov theory (Astrom and Wittenmark, 1995). These controllers are not discussed in this report.

4.2 Proportional controller

For the proportional controller it is assumed that the reference trajectory can be decomposed in the $X-Y$ plane in terms of straight-line segments and arcs. In the first case that is illustrated in Figure 3, a $X-Y$ plane is shown in which the reference trajectory is the X axis itself and the vehicle is initially at (x_p, y_p, ϕ). Whenever the reference trajectory is a straight-line segment, the vehicle position can be expressed in terms of the coordinates of Figure 3 and then the correcting control signal can be computed as shown below.

The linear orthogonal displacement Γ and angular deviation Θ can be determined from the actual vehicle

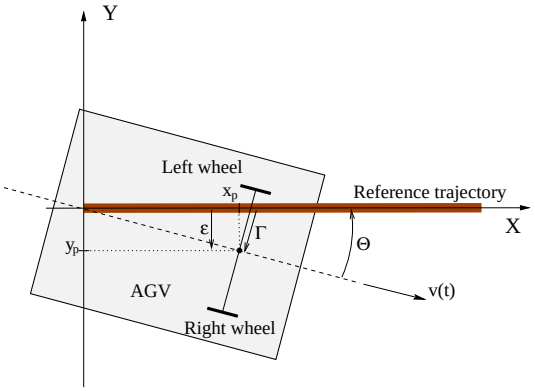

Figure 3. Trajectory deviation for straight-line segments.

position by:

$$\Theta(t) = -\phi_p(t),$$

$$\Gamma(t) = \frac{y_p(t)}{\cos\phi_p(t)}.$$

Using the above relationships together with the vehicle kinematic model Eqs. (1), (2) and (3), the following differential equations can be derived to describe the behaviour of the vehicle deviation:

$$\dot{\Gamma}(t) = -\left(\frac{r\Gamma(t)\left(\omega_r(t)-\omega_l(t)\right)}{b} + v(t)\right)\tan\Theta(t)$$

$$\dot{\Theta}(t) = -\frac{r\left(\omega_r(t)-\omega_l(t)\right)}{b}.$$

Using Eqs. (7) and (8) and considering $v(t) = v_p$, we can write

$$\dot{\Gamma}(t) = -\left(\frac{2r\Gamma(t)\Delta\omega(\Gamma(t),\Theta(t)) + bv_p}{b}\right)\tan\Theta(t),$$

$$\dot{\Theta}(t) = -\frac{2r}{b}\Delta\omega(\Gamma(t),\Theta(t)).$$

The above model can be further simplified by rewriting it in terms of $\varepsilon(t) = \Gamma(t)\cos\Theta(t) = y_p(t)$. The simplified model is given by:

$$\dot{\varepsilon}(t) = v_p\sin\Theta(t), \tag{12}$$

$$\dot{\Theta}(t) = -\frac{2r}{b}\Delta\omega(\Gamma(t),\Theta(t)). \tag{13}$$

The proportional control law may be defined as:

$$\Delta\omega(\Gamma(t),\Theta(t)) = K_\varepsilon(t)\varepsilon(t) + K_\Theta\Theta(t) \tag{14}$$

in which $K_\varepsilon(t) = K_\Gamma/\cos\Theta(t)$. By placing the proportional control law into the simplified model given by (12) and (13) we find that

$$\dot{\varepsilon}(t) = v_p\sin\Theta(t),$$

$$\dot{\Theta}(t) = -\frac{2r}{b}(K_\varepsilon(t)\varepsilon(t) + K_\Theta\Theta(t)).$$

which represents an autonomous dynamic and nonlinear system that has $(\varepsilon,\Theta) = (0,0)$, $(\varepsilon,\Theta) = (-K_\Theta\pi/K_\Gamma,\pi)$ and $(\varepsilon,\Theta) = (K_\Theta\pi/K_\Gamma,-\pi)$ as attractors. The first attractor $(\varepsilon,\Theta) = (0,0)$ is stable in the

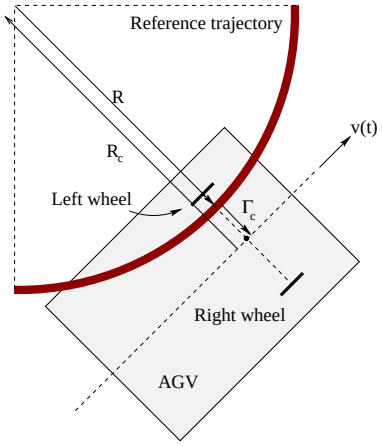

Figure 4. Trajectory deviation for soft arcs.

sense of Lyapunov for K_Θ and K_Γ being positive constants. The other two attractors imply that the vehicle is following the reference trajectory with a constant orthogonal displacement but in the opposite direction. However, considering that the initial condition is restricted to $|\Theta| < \pi/2$ then the vehicle had to make an u-turn in order to move in the opposite direction and eventually Θ becomes $\pi/2$ which would result in a failure of the trajectory detecting sub-system and will stop the vehicle.

Supposing that the vehicle is sufficiently aligned with the reference trajectory $\sin\Theta \approx \Theta$, $K_\varepsilon \approx K_\Gamma$, then the system dynamics can be described by

$$\begin{pmatrix} \dot{\varepsilon}(t) \\ \dot{\Theta}(t) \end{pmatrix} = \begin{pmatrix} 0 & v_p \\ -2rK_\Gamma/b & -2rK_\Theta/b \end{pmatrix} \begin{pmatrix} \varepsilon(t) \\ \Theta(t) \end{pmatrix}.$$

The transient response in this case is determined by the roots of

$$s^2 + \frac{2rK_\Theta}{b}s + \frac{v_p 2rK_\Gamma}{b} = 0.$$

It is desired that the vehicle movement toward the marked trajectory be smooth, fast and without overshoot. To achieve these specifications $K_\Theta > 0$ and

$$K_\Theta = +\sqrt{\frac{2v_pK_\Gamma b}{r}}, \tag{15}$$

which implies that the closed-loop is stable with two equal roots given by

$$s_{1,2} = -\frac{r}{b}K_\Theta. \tag{16}$$

From Eqs. (15) and (16), the gains K_Γ and K_Θ can be determined to provide the desired dynamic response. However, this design procedure can result in a controller which may not provide satisfactory performance while the vehicle is moving along the curvilinear paths. Thus the design of the controller should also take into account the performance along the curved paths with constant radius R as shown in Figure 4. Considering the vehicle has attained the steady-state, the radius of the curve traversed by the vehicle is given by (9). It can be easily verified that for the vehicle to track the radius of curvilinear trajectory it is required that $\Delta\omega(\Gamma(t),\Theta(t)) \neq 0$ but in steady-state $\Theta(t) = 0$. However, during its movement along the curve the proportional controller would provide a constant and non-zero orthogonal displacement. Intuitively we can find that such displacement $\Gamma_c > 0$ will be positive for the curve to the left and, according to Figure 4, $\Gamma_c = -(R_c + R)$. Using Eq. (9) this displacement can be expressed by

$$\Gamma_c = \frac{v_p}{\Delta\omega(\Gamma,0)}\frac{b}{2r} - R, \tag{17}$$

with

$$\Delta\omega(\Gamma,0) = K_\Gamma\Gamma_c.$$

Then, the orthogonal displacement Γ_c in steady-state is given by the solution of

$$\Gamma_c^2 + \Gamma_c R - \frac{v_p b}{2rK_\Gamma} = 0.$$

Since $\Gamma_c > 0$, the physically acceptable solution is

$$\Gamma_c = \frac{1}{2}\left(-R + \sqrt{R^2 + 2\frac{v_p b}{rK_\Gamma}}\right).$$

and thus K_Γ can be determined in terms of the deviation from curvilinear trajectory by:

$$K_\Gamma = \frac{2v_p b}{r\left((R+2\Gamma_c)^2 - R^2\right)}. \tag{18}$$

Thus the design of the proportional controller needs the specification of the permissible deviation from the curved trajectory. Moreover, from (18) and (15) the values of K_Γ and K_Θ can be determined.

5 Simulation

Two simulation studies were carried out in order to evaluate the proportional controller design. In doing so, the proportional controller was designed to give $\Gamma_c = 0.01m$ and $\Gamma_c = 0.02m$, according to Eqs. (18) and (15). The corresponding controllers are named on CP-1 and CP-2, respectively. The simulated trajectory is shown in Figure 5. In order to allow further comparisons, the experimental setup presented on the next section uses the same reference trajectory. In this simulation the AGV must follow the trajectory and some strategic points are marked as *A*, *B*, *C*, *D*, *E*, *F*, *G*, *H* and *I*. The arcs have a radius of $R = 0.3\ m$. The vehicle cruising speed was $v_p = 0.1625\ m/s$ and the AGV parameters are the same of the prototype vehicle. The AGV starts with an initial trajectory deviation of $\Gamma = 1$ *cm* and $\Theta = 0$.

Figures 6 and 7 present the plots of Γ and Θ of the AGV for the controllers CP-1 and CP-2, respectively. In these plots, small circles indicate the instants when

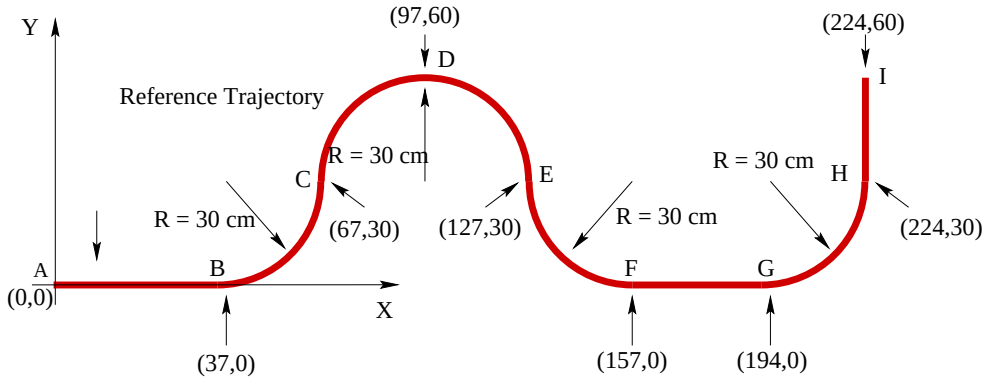

Figure 5. Reference trajectory used for simulation and experimental evaluation (coordinates in centimeters).

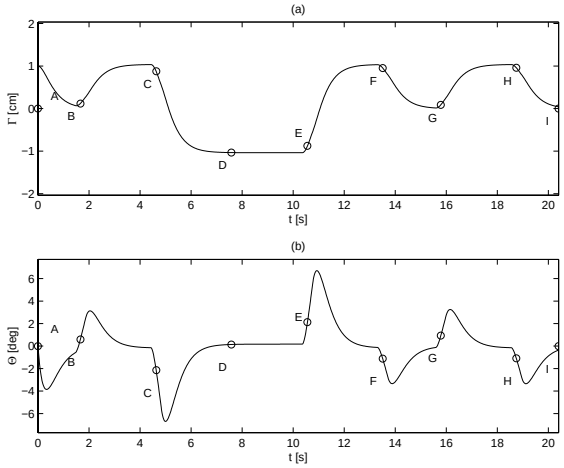

Figure 6. Simulation results for the proportional controller with $\Gamma_c = 0.01m$: (a) Γ and (b) Θ.

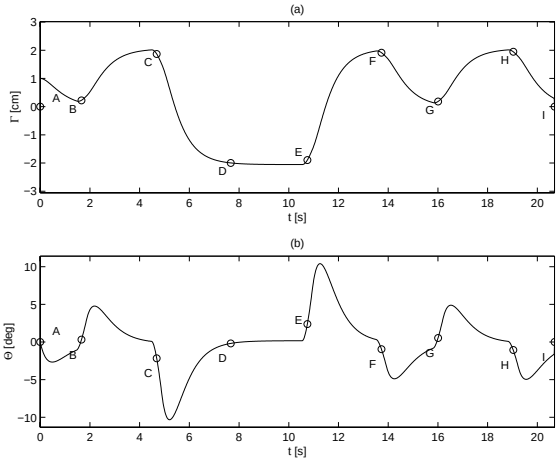

Figure 7. Simulation results for the proportional controller with $\Gamma_c = 0.02m$: (a) Γ and (b) Θ.

the vehicle was close to each marked positions from *A* to *I*. It can be seen that the steady-state values for Γ (Γ_c) for each controller was correctly verified in the soft arcs (segments *B-F* and *G-H)*, and the stabilization to zero of Γ and Θ occurred without overshoot for the straight-line segments (*A-B*, *F-G*, and *H-I*). From Eqs. (18) and (15), it can be verified that for reducing Γ_c, the gains K_Γ and K_Θ should increase. For large values of K_Γ and K_Θ, the proportional controller may be very sensitive to noise in the estimation of Γ and Θ. Moreover, the controller CP-1 is faster than the controller CP-2. This fact can also be verified from the real poles given by Eq. (16), once K_Θ is smaller for CP-2 than for CP-1. Therefore, a compromise between convergence speed and noise sensitivity must be taken into account for the design of this controller.

6 Experimental results

In order to evaluate the trajectory controller, experimental tests were carried out with a trajectory identical to the one used in the simulation studies (see Figure 5).The initial trajectory error was $\Gamma = 1$ *cm* and $\Theta = 0$**.** The vehicle stops at *I* when the trajectory fault is detected. A trajectory fault occurs when the deviation is out of the bounds given by eqs. (5) and (6).

The proportional controller is designed in order to have $\Gamma_c = 0.02m$ (CP-2 in Section 5) for curvilinear segments. According to Eqs. (18) and (15), this results in $K_\Gamma = 107.42$ and $K_\Theta = 17.18$. Considering the size and weight of the AGV, the navigating velocity is chosen as $v_p = 0.1625m/s$.

The experimental results for the proportional controller are shown in Figure 8. In this figure, Γ and Θ of the controlled AGV are plotted versus the time and the corresponding values when the AGV passed from mark *A* to *I* are represented by small circles. As can be seen in Figure 8(a), Γ remained limited to $\pm 0.02m$ in the arcs *B-C*, *E-F* and *G-H*. For the arc *C-D-E*, some oscillations occurred giving a $\Gamma \neq \Gamma_c$. However, these oscillations were not observed in arcs *B-C*, *E-F* and *G-H*. In fact, this can be explained by the nonlinearities of the right wheel mechanical system. As the right wheel velocity controller has some difficulty to stabilize at low velocities, the result is an unstable behaviour in the arc *C-D-E*. Figure 8(b) shows that Θ has been kept small for all trajectory with some peaks in the beginning of the arcs. This same behaviour was also observed in the simulation as presented in Section 5. However, we can verify a small offset in Θ and small oscillations in Γ. This may be a result of the sensor misalignment, as it can be verified by a fur-

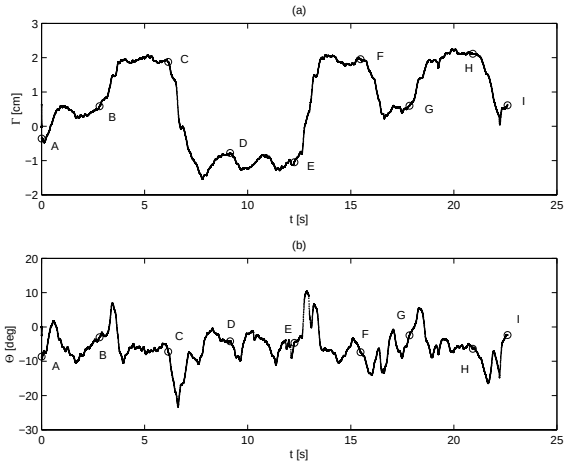

Figure 8. Experimental results for the proportional controller: (a) Γ and (b) Θ of the controlled vehicle.

ther analysis of equations (12) and (13). In doing so, the control law $\Delta\omega$ employs sensor readings Γ_s and Θ_s given by

$$\Gamma_s = \Gamma + \delta\Gamma,$$
$$\Theta_s = \Theta + \delta\Theta,$$

with $\delta\Gamma$ and $\delta\Theta$ being the sensor error components due to misalignment. As a consequence the system attractor and the sensor readings will be different from zero. It can be observed that the simulations presented in Section 5 used a perfect sensor model without errors on the readings of Γ and Θ, and the controller provided the ideal steady-state for straight-line segments: $\Gamma = 0$ and $\Theta = 0$.

7 Conclusion

We have presented the design of a proportional output feedback trajectory controller for a differential drive Automated Guided Vehicle (AGV). Its control architecture assumes that the two drive wheels are not coupled and the vehicle dynamics is not taken into account. It employs two independent velocity controllers that ensure the wheels velocities defined by the trajectory controller. The reference trajectory is painted on the ground and consists of only straight line segments and soft arcs. The controller parameters were analytically determined as a function of the vehicle parameters and of the specified trajectory error behaviour. Simulated and experimental results have shown the satisfactory performance of the proposed controller.

8 Acknowledgment

The authors thank the CNPq (*Conselho Nacional de Desenvolvimento Científico e Tecnológico*) for the award of research and study fellowships during the course of these investigations.

References

Aguilar, M., Souères, P., Courdesses, M. and Fleury, S. (1998). Robust path-following control with exponential stability for mobile robots, *Proceedings of the IEEE Int. Conf. on Robotics and Automation* pp. 3279–3284.

Astrom, K. and Wittenmark, B. (1995). *Adaptive Control*, 2nd edn, Prentice-Hall, Inc., Englewood Cliffs, N.J.

Borges, G., Lima, A. and Deep, G. (1998). Characterization of a neural network-based trajectory recognition optical sensor for autonomous vehicles, *Proceedings of the IEEE Int. Conf. on Instrumentation and Measurement* pp. 1179–1184.

Colbaugh, R., Barany, E. and Glass, K. (1998). Adaptive control of nonholonomic robotic systems, *Journal of Robotic Systems* **17**(7): 365–393.

Cox, I. J. (1991). Blanche - an experiment in guidance and navigation of an autonomous robot vehicle, *IEEE Transactions on Robotics and Automation* **7**(2): 193–204.

d'Andréa Novel, B., Campion, G. and Bastin, G. (1995). Control of nonholonomic wheeled mobile robots by state feedback linearization, *The International Journal of Robotics Research* **14**(6): 543–559.

Fung, Y. and Tso, S. (1998). Analysis of linguistic fuzzy control for curved-path-following autonomous vehicles, *Proceedings of the IEEE Int. Conf. on Robotics and Automation* pp. 2506–2511.

Mazur, A. and Hossa, R. (1997). Universal adaptive λ - tracking controller for wheeled mobile robots, *In Proceedings of the IFAC Symposium on Robot Control* pp. 33–38.

Tso, S., Fung, Y. and Cheung, Y. (1996). Fuzzy logic control for differential wheel drive agvs using linear optosensor arrays, *Proceedings of the IEEE Int. Conf. on Robotics and Automation* pp. 2816–2821.

Zhang, Y., Velinsky, S. and Feng, X. (1997). On the tracking control of differentially steered wheeled mobile robots, *Journal of Dynamic Systems, Measurement, and Control - ASME* **119**: 455–461.